



1/f Noise in Human Cognition

D. L. Gilden; T. Thornton; M. W. Mallon

Science, New Series, Vol. 267, No. 5205 (Mar. 24, 1995), 1837-1839.

Stable URL:

<http://links.jstor.org/sici?sici=0036-8075%2819950324%293%3A267%3A5205%3C1837%3A1NIHC%3E2.0.CO%3B2-4>

Your use of the JSTOR archive indicates your acceptance of JSTOR's Terms and Conditions of Use, available at <http://www.jstor.org/about/terms.html>. JSTOR's Terms and Conditions of Use provides, in part, that unless you have obtained prior permission, you may not download an entire issue of a journal or multiple copies of articles, and you may use content in the JSTOR archive only for your personal, non-commercial use.

Each copy of any part of a JSTOR transmission must contain the same copyright notice that appears on the screen or printed page of such transmission.

Science is published by American Association for the Advancement of Science. Please contact the publisher for further permissions regarding the use of this work. Publisher contact information may be obtained at <http://www.jstor.org/journals/aaas.html>.

Science

©1995 American Association for the Advancement of Science

JSTOR and the JSTOR logo are trademarks of JSTOR, and are Registered in the U.S. Patent and Trademark Office. For more information on JSTOR contact jstor-info@umich.edu.

©2003 JSTOR

with a band of 29 kD). A fourth mAb was found that did not react with standard immunoblots but did bind to intact vesicles (VSP4D). Ascites production, immunoglobulin G (IgG) purification, and Fab fragment isolation were performed according to standard procedures (17). For quantitation of antibody binding to CW vesicles, the vesicles were mixed with 3% bovine serum albumin (BSA) (fatty acid-free; Sigma) for 1 hour at 4°C. Vesicles (10 to 20 µg of vesicle proteins) in a total volume of 200 µl were mixed overnight at 4°C with 0.2 to 0.3 mg of antibodies (ascites) per milliliter or a control mouse IgG. Each sample was layered onto a three-step sucrose gradient (100 µl of 15%, 200 µl of 10%, and 200 µl of 5% sucrose in homogenization buffer) and centrifuged at 4°C for 20 min with an SW-55Ti rotor at 192,000g. The supernatant and the sucrose were removed completely and the pellet was resuspended in 25 µl of electrophoresis sample buffer (18) with an additional 1% SDS and analyzed as described (5). The effect of antibody on motor binding to vesicles was measured with VSP4D and VSP2B (control) as described (5, 7) with slight modification. CW vesicles (2.0 to 3.0 µg of vesicle proteins for kinesin binding and 5 µg for dynein binding) in a total volume of 60 µl of PMEE' buffer [35 mM K-Pipes (pH 7.4), 5 mM MgCl₂, 5 mM EGTA, and 0.5 mM EDTA] were mixed with IgG (0.16 to 0.25 mg/ml for kinesin binding and 0.42 mg/ml for dynein binding) on ice for 1 hour and 10 to 15 min at 37°C before addition of a purified motor fraction [10 to 20 nmol of motors prepared as described in (8)]. The binding experiments were performed as described (5). Binding of motors was inhibited by VSP4D, whereas no effect was observed with VSP2B.

20. The *in vitro* vesicle motility assay on polar microtubules was performed after preparation of cytosolic fractions and CW chick embryo fibroblast vesicles as described (8, 11). Sea urchin sperm axonemes were a gift from T. Salmon (University of North Carolina at Chapel Hill, NC). Porcine tubulin (1×) and *N*-ethylmaleimide-treated tubulin (2×) were mixed and diluted to ~3.0 mg/ml final concentration with PMEE' and 1 mM guanosine triphosphate (GTP). Axonemes were added to an acid-washed cover slip in a flow cell formed with two parallel strips of double-sided tape and a glass slide for 2 min at a concentration of ~2 per video field (~500 µm²). The tubulin mixture was exchanged into the flow cell and incubated in a humidity chamber at 37°C for 15 min. The free tubulin was washed out with PMEE', 1 mM GTP, and 20 µM Taxol. CW vesicles (0.2 mg/ml) were reacted with mAbs (0.1 mg/ml) for 2 to 3 hours with rocking at 4°C. To measure motility, we incubated the mixture of vesicles and antibodies with a cytosolic fraction (S3) and 5 mM Mg-ATP, and then added the mixture to the polarized microtubules in a flow cell. Samples were observed on a heated Zeiss Axiovert-100 microscope at 35° to 37°C by video-enhanced differential interference contrast, and motility was analyzed as described (5). The number of vesicle movements was normalized to the concentration of vesicles in the medium and the length of microtubules in the field [expressed as movements per minute per 36 µm of microtubule length (per 70 vesicles in 4 µm² of buffer per minute)]. Moving vesicles are counted only once after they bind and move (stopping and restarting is not counted as a second movement). Vesicles do not reverse direction of movements. Means and standard error of means (SEM) were calculated and weighted by the number of minutes analyzed for each field.
21. To identify the antigen for VSP4D, we biotinylated CW vesicles as described (7). Biotinylated vesicles were collected at a 15/60% sucrose interface after centrifugation at 192,000g for 30 min (Beckman SW55Ti rotor) and were dialyzed against PMEE' before incubation with 3% BSA at 4°C for 1 hour. The vesicles were then mixed with the designated antibody for 5 hours at 4°C and collected at a 15/60% sucrose interface after centrifugation. The vesicles were solubilized with 1% Triton X-100 and 0.5 M NaCl and centrifuged at 150,000g for 30 min in a TLA100.2 rotor. The supernatants were incubated with protein A-Sepharose CL-4B (Schleicher & Schuell) for 4 to 5 hours at 4°C and washed four times with NET buffer [150 mM NaCl,

50 mM Tris-HCl, 5 mM EDTA (pH 8.0)]. The immunoprecipitates were solubilized directly in electrophoresis sample buffer (18) and analyzed by SDS-polyacrylamide gel electrophoresis (PAGE) and immunoblotting.

22. E. R. Steuer, L. Wordeman, T. A. Schroer, M. P. Sheetz, *Nature* **345**, 266 (1990).
23. We thank J. Lockman for assisting in mAb produc-

tion, J. McIlvain for help with microscopy, and Z. Wang for help with the motility assay. We also thank J. Lippincott-Schwartz and H. P. Erickson for comments on the manuscript, and members of the Sheetz lab for discussions. Supported by grant NS 23345 from the National Institutes of Health.

19 September 1994; accepted 9 December 1994

1/f Noise in Human Cognition

D. L. Gilden,* T. Thornton, M. W. Mallon

When a person attempts to produce from memory a given spatial or temporal interval, there is inevitably some error associated with the estimate. The time course of this error was measured in a series of experiments where subjects repeatedly attempted to replicate given target intervals. Sequences of the errors in both spatial and temporal replications were found to fluctuate as 1/f noises. 1/f noise is encountered in a wide variety of physical systems and is theorized to be a characteristic signature of complexity.

Of the types of activity that characterize physical systems, perhaps the most ubiquitous and puzzling is the appearance of 1/f noise, a form of temporal fluctuation that has a power density inversely proportional to the frequency (that is, power ~ 1/f). 1/f noise, also known as pink or flicker noise, varies with a predictability intermediate between white noise (no correlation in time, power ~ 1/f⁰) and Brownian motion (no correlation between increments, power ~ 1/f²). 1/f noise has been observed in a profusion of domains as diverse as condensed matter systems (1, 2), traffic flow (3), quasar emissions (4), river discharge (5), DNA base sequence structure (6), and cellular automata (7). This list is hardly exhaustive, as entire symposia are devoted to its occurrence and causation (8). The universality of 1/f noise suggests that it does not arise as the consequence of particular physical interactions, but instead is a general manifestation of complex systems. Here we present evidence that 1/f noises are associated with certain basic aspects of human cognition: the representation of spatial and temporal intervals.

Despite the interest in complex systems within the social sciences, there have been few examples of 1/f noise reported in human or animal behavior (9). Most notably, music and speech have been shown to have 1/f fluctuations in both pitch and loudness (10). The occurrence of 1/f noise in these contexts, however, should be distinguished from its appearance in purely physical systems. Pitch and loudness carry information in music and speech signals and are therefore subject to the constraints that exist generally in communication. Their spectral

properties may be due to the fact that 1/f noise represents an optimal compromise between efficient transfer of information (maximized by white noise) and immunity to error (6).

Our investigations concern the production of spatial and temporal intervals. The experiments we conducted were extremely simple. Subjects were first given an example of a target spatial or temporal interval and then made, to the best of their ability, a series of replicates. The errors in replication were treated as a time series and were submitted to Fourier analysis. Figure 1 illustrates the power spectra of the errors deriving from the estimation of temporal intervals. Results from six experiments are displayed in which the target time interval varied between 0.30 and 10 s in duration (Fig. 1A). These power spectra share a family resemblance that is distinguished by the presence of two features. All the spectra are 1/f at frequencies less than about 0.2 Hz, and there is a quadratic trend at higher frequencies that becomes progressively more pronounced with shorter target durations.

The overall coherence of this data set suggests that it may be understood in terms of a few simple mechanisms. Earlier work on timing variance (11) presented evidence for a model in which the production of temporal intervals is composed of two parts: an internal clock (C) that mediates the judgment of time passage, and a motor program that actuates the responses which signal the beginning and ending of each interval. The motor program in this model does not operate instantaneously, and all responses have an assigned motor delay (MD). In terms of these two components, the *j*th observed interval *I_j* is written as

$$I_j = C_j + MD_j - MD_{j-1}$$

The difference in motor delays arises from

Department of Psychology, University of Texas at Austin, Austin, TX 78712, USA.

*To whom correspondence should be addressed.

the particular boundary condition typically used in timing studies: the ending of the ($j - 1$)st interval is also the beginning of the j th interval. Previous investigations of this model (11, 12) did not focus on the sequential structure of interval production, and both the internal clock and the motor program were regarded as sources of random white noise, albeit with possibly different variances. The data in Fig. 1A make it clear that sequences of errors in duration judgment are not white noises composed of uncorrelated increments, but instead appear to be a mixture of at least two types of noise (13). We have found that the entire data set can be simulated by regarding the internal clock as a source of $1/f$ noise while maintaining the notion that the motor program generates uncorrelated white noise.

In this two-component approach there is one free parameter, the ratio of clock root-mean-square (rms) error to motor rms error. We have allowed this parameter to vary freely in fitting the model to data. Figure 1B displays the optimal fits together with the error ratios. This model captures many of the important features of the data set: the $1/f$ portion at low frequencies, the gradual formation of the quadratic trend with decreasing target duration, and the existence of a characteristic frequency near 0.2 Hz where the spectrum turns up (14). The model accounts for the high-frequency increase in power in terms of the two roles that a given motor delay plays. The ($j -$

1)st motor delay simultaneously lengthens the ($j - 1$)st interval and shortens the j th interval. A consequence of this coupling is that long intervals tend to be followed by short intervals and vice versa. The resultant high-frequency alternation in the time domain forms the quadratic trend in the power spectrum (15).

The demonstration of $1/f$ noise in an isolated perceptual domain raises the issue of its generality. As shown by the data in Fig. 2, errors in the repeated production of a fixed spatial interval also generate a time series with a $1/f$ power spectrum. The shape of this spectrum is similar to that produced by the reckoning of time intervals greater than 1 s. The line length spectrum is exactly $1/f$ for frequencies less than 0.1 and then whitens at higher frequencies. As was found in the time domain, the spectrum appears to be formed from two sources: a $1/f$ noise that derives from perceptual judgment, and a white noise that is associated with pointing errors produced by pen placement (16). Evidently the production of temporal intervals is not privileged with respect to the manifestation of $1/f$ noise.

In a final experiment, the power spectra of reaction time sequences were studied. Reaction time differs from the conscious production of a time interval in one obvious but important way: The magnitude is not intentional. In our experiment, subjects depressed the space bar on a computer keyboard as rapidly as possible after the presen-

tation of a visual stimulus. If $1/f$ noises are associated with the controlled aspects of interval production, then they should be absent from reaction time. Furthermore, because reaction time intervals are measured as the temporal asynchrony between the onset of a visual display and the response, we would not expect to see the growth in power that was observed at high frequencies in the production of temporal intervals. This feature only arises when a single response signals both the ending of one interval and the beginning of the next. Figure 3 shows the power spectrum of reaction-time sequences. As expected, it is fairly constant across the resolved span of frequency. We conclude that $1/f$ noises arise from cognitive mechanisms that mediate the judgment of magnitude, independent of whether the magnitude exists in time or in space.

Fig. 1. (A) Spectral power densities, S_k , for six experiments in the estimation of time duration (19). The data from these experiments were sequences of errors, d_n , in estimates of a given target duration, T_0 . T_0 varied across experiments and is shown adjacent to each spectrum (in seconds). S_k was computed (20) with overlapping samples of $N = 2m$ data points according to

$$S_k = \left| \sum_{n=0}^{N-1} d_n e^{2\pi i k n / N} \right|^2$$

Because responses in each experiment were initiated at intervals characterized by T_0 , frequency (in Hertz) is computed as $f_k = (k - 1)/(2mT_0)$, for $k = 1, 2, 3, \dots, m$. In order to minimize the variance of the spectral estimates, we used two values of m : $m = 256$ at low frequencies ($f_k < 0.02/T_0$) and $m = 32$ at high frequencies ($f_k \geq 0.02/T_0$). The spectral density (in milliseconds squared) is normalized within each experiment so that the total power equals the mean square amplitude

$$\left(\frac{1}{N} \sum_{n=0}^{N-1} d_n \right)^2$$

Also shown is a line depicting an exact $1/f$ power spectrum. Descending from top to bottom, at frequencies $f_k < 0.1$ Hz, best fit lines to the power spectra had slopes of $-1.1, -1.0, -1.1, -0.90, -1.2,$ and -0.94 , respectively. **(B)** Best fits to the data from a simple model that represents the production of time intervals as being composed of an internal clock that generates $1/f$ noise and a motor delay that produces white noise as normally distributed deviates. The different curves are indexed by the ratio of the rms clock noise to the rms motor noise. This ratio is given next to each curve and is observed to increase linearly with the target duration.

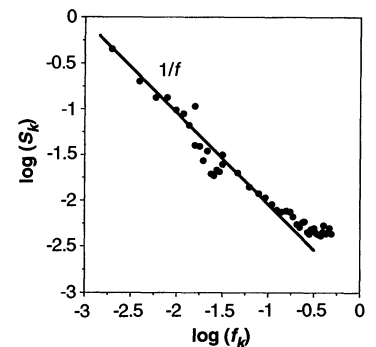
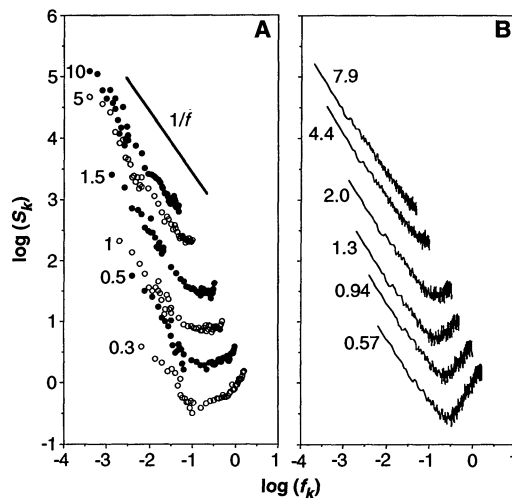


Fig. 2. The spectral power density, S_k , is shown for errors in the estimation of a 1-inch spatial interval (21). The method of analysis was exactly as for the timing experiments. Because there was no characteristic time interval separating responses in this experiment, frequency is computed as $f_k = (k - 1)/(2m)$, for $k = 1, 2, 3, \dots, m$. The power spectrum is normalized so that the total power equals the mean square amplitude (in millimeters squared). Also shown is a line depicting an exact $1/f$ power spectrum.

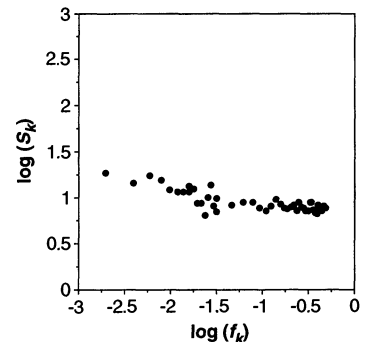


Fig. 3. The spectral power density, S_k , is shown for sequences of reaction time (22). The method of analysis was exactly as for the timing experiments. Frequency is computed as $f_k = (k - 1)/(2m)$, for $k = 1, 2, 3, \dots, m$. The power spectrum is normalized so that the total power equals the mean square amplitude (in milliseconds squared).

The discovery of $1/f$ noise in human judgment suggests that the theory of complex systems may have application within cognitive science. Although the etiology of $1/f$ noise remains controversial, it appears to be associated with systems that relax upon perturbation with no preferred spatial or temporal scales (2). There are a number of frameworks that have been proposed to account for the ubiquity of systems displaying scale freedom. In particular, the theory of self-organized criticality (17) and the notion that $1/f$ noises arise from sequences of contingent processes (18) are two that are potentially relevant to psychophysics. The data presented here raise the possibility that cognition has formal or physiological organizations that are common to complex dynamical systems.

REFERENCES AND NOTES

1. P. Dutta and P. M. Horn, *Rev. Mod. Phys.* **53**, 497 (1981).
2. M. B. Weissman, *ibid.* **60**, 537 (1988).
3. T. Musha and H. Higuchi, *Jpn. J. Appl. Phys.* **15**, 1271 (1976).
4. W. Press, *Comments Astrophys.* **7**, 103 (1978).
5. B. B. Mandelbrot and J. R. Wallis, *Water Resour. Res.* **4**, 909 (1968).
6. R. F. Voss, *Phys. Rev. Lett.* **68**, 3805 (1992).
7. K. Christensen, Z. Olami, P. Bak, *ibid.*, p. 2417.
8. P. H. E. Meijer, R. D. Mountain, R. J. Soulen Jr., Eds., *Sixth International Symposium on Noise in Physical Systems* (National Bureau of Standards, Washington, DC, 1981); C. M. Van Vleit, Ed., *Ninth International Symposium on Noise in Physical Systems* (World Scientific, Singapore, 1987).
9. The paucity of spectral analyses of noise in experimental psychology may reflect the way in which noise is regarded in typical experimental designs. Standard approaches focus on the variance associated with treatment effects and regard the residual error as homogeneous and essentially uninteresting. Different methodologies and designs are required when the noise is instead the focus of interest. In this case, an unusual but appropriate methodology is to remove the variance induced by the presentation of different stimuli and to measure the fluctuations that occur as a subject responds to a single, constant stimulus. This type of design was common in the early days of sensory psychophysics when investigators often employed a time-invariant stimulus to study fluctuations at threshold [J. P. Guilford, *Am. J. Psychol.* **38**, 534 (1927)]. The fluctuations we measure are similar to those studied by early psychophysicists in that they arise spontaneously in the course of cognitive activity.
10. R. F. Voss and J. Clarke, *Nature* **258**, 317 (1975); *J. Acoust. Soc. Am.* **63**, 258 (1978).
11. A. M. Wing, in *Tutorials in Motor Behavior*, G. E. Stelmach and J. Requin, Eds. (North-Holland, Amsterdam, 1980), pp. 469–486; A. M. Wing and A. B. Kristofferson, *Percept. Psychophys.* **14**, 5 (1973).
12. S. W. Keele, in *Handbook of Perception and Human Performance*, K. Boff, L. Kaufman, J. Thomas, Eds. (Wiley, New York, 1986), vol. 2, pp. 30.1–30.60.
13. The errors associated with interval production have been analyzed with respect to their distributional properties. In every case the error distributions were indistinguishable from a Gaussian. This observation underscores the relevance of regarding experimental error in terms of a time series. Error distributions may conform to the standard assumptions of parametric statistics, and yet the time development of the error may not be a random white noise.
14. The model and data were also consistent with respect to the functional relation between the magnitudes of the replication errors and the target intervals. A measure of error growth is the Weber fraction, in this context defined by the ratio of the rms error to the target duration. Although there is conflicting evidence concerning the existence of constant Weber fractions (rms error proportional to the target duration) in the production of temporal intervals [L. G. Allan, *Percept. Psychophys.* **26**, 340 (1979); J. H. Wearden, *Learn. Motiv.* **22**, 59 (1991)], such a proportionality was found in these data ($r^2 = 0.99$); there is a constant Weber fraction across the entire data set of 0.05. The model also exhibited a linearity in error growth in that optimal fits to the data specified a ratio of rms clock error to rms motor error that was proportional to the target duration ($r^2 = 0.99$). While there is some ambiguity in making inferences from the time dependence of this error ratio, the variability associated with the motor delay is expected to be independent of the magnitude of the target interval (11, 12), and it appears as if the internal clock generates a constant Weber fraction.
15. The differential error growth in the clock and motor components accounts for the increasing prominence of the quadratic trend with decreasing target duration. When the target interval is large, say 5 or 10 s, the amplitude of the clock error exceeds that of the motor delay, and the $1/f$ clock noise masks the spectral effects due to response initiation. As the error ratio approaches unity at shorter target intervals, the quadratic trend becomes visible at high frequencies. At sufficiently short target durations, there is convergence of the spectra in the quadratic regime.
16. Discrimination accuracy in visual perception is often governed by constant Weber fractions [E. G. Boring, H. S. Langfeld, H. P. Weld, *Foundations of Psychology* (Wiley, New York, 1948)], and we anticipate that varying the magnitude of the target interval would have roughly the same effect on the spectra of spatial intervals as it did for temporal intervals. However, the power spectra of spatial interval sequences are not expected to turn up at high frequencies as they did for temporal interval sequences. This feature exists for temporal intervals because of the traditional design used in timing studies: the end of one interval is the beginning of the next. In the design we employed for the production of spatial sequences, the interval boundaries were not coupled.
17. P. Bak, *Physica A* **163**, 403 (1990); *ibid.* **191**, 41 (1992); P. Bak, C. Tang, K. Wiesenfeld, *Phys. Rev. Lett.* **59**, 381 (1987); *Phys. Rev. A* **38**, 364 (1988); P. Bak, K. Chen, M. Creutz, *Nature* **342**, 780 (1989); K. L. Babcock and R. M. Westervelt, *Phys. Rev. Lett.* **64**, 2168 (1990); H. J. Jensen, *ibid.*, p. 3103.
18. E. W. Montroll and M. F. Shlesinger, *Proc. Natl. Acad. Sci. U.S.A.* **79**, 3380 (1982); B. J. West and M. F. Shlesinger, *Int. J. Mod. Phys. B* **3**, 795 (1989).
19. In the temporal interval experiments, subjects were given a 1-min sample of the target interval with a metronome. They then attempted to reproduce the interval by pressing the spacebar on a computer keyboard. This was done repeatedly over a large number of trials without feedback. Subjects were free to count if they felt that would help them give more accurate estimates of the longer intervals. It may not be possible to prevent counting and still allow subjects to attend to the production task. A given response served as both the ending of the ($j - 1$)st interval and the beginning of the j th interval. The number of trials was 1000 for all timing experiments, except for the 10-s trials for which the number was 400. Timing error was about 4 ms. Data shown represents the average over six subjects. Each subject contributed one sequence at each target duration. The same subjects participated in all experiments.
20. W. H. Press, S. A. Teukolsky, W. T. Vetterling, B. P. Flannery, *Numerical Recipes in FORTRAN* (Cambridge Univ. Press, New York, ed. 2, 1992), pp. 550–551.
21. Subjects in the spatial interval study made 1000 successive estimations of a 1-inch displacement on a GTCO Digi-Pad-5 digital tablet. Data shown represent the average over six subjects with each subject contributing one sequence. In this experiment subjects placed a pen at the intersection of a cross hair and then placed the pen at what they estimated to be 1 inch. The Euclidean distance was computed to obtain the estimated distance. No feedback was given. Distance measurement on the digital tablet is accurate to 0.001 inch.
22. In the reaction-time experiment, a stimulus was visually presented at random time intervals on a computer monitor. As soon as the stimulus appeared, the subject hit the spacebar as quickly as possible. Reaction times were computed as the asynchrony of the response from the onset of the visual stimulus and had a mean of about 100 ms. Data shown represent the average over six subjects with each subject contributing one sequence of 1000 reaction times. Timing error was about 4 ms.
23. We wish to acknowledge helpful conversations with T. Tajima, L. Willerman, L. Cohen, B. Spellman, and R. Diehl. The digital tablet was programmed by L. Stern. Supported in part by Air Force Office of Scientific Research grant 749620-93-1-0307.

2 September 1994; accepted 23 January 1995